Published in final edited form as:
Neuron. 2007 February 15; 53(4): 487–493.

The Diffusible Calcium Sensor, Hippocalcin, Gates the Calcium Activation of the Slow Afterhyperpolarization in Hippocampal Pyramidal Neurons

Anastassios V. Tzingounis[1], **Masaaki Kobayashi**[3], **Ken Takamatsu**[3], and **Roger A. Nicoll**[1,2,*]

1 *Department of Cellular and Molecular Pharmacology, University of California San Francisco, CA 94143,*

2 *Department of Physiology, University of California San Francisco, CA 94143*

3 *Department of Physiology, Toho University School of Medicine, 5-21-16 Ohmori-nishi, Ohta-ku, Tokyo 143-8540, Japan*

SUMMARY

In the brain, calcium influx following a train of action potentials activates potassium channels that mediate a slow afterhyperpolarization current (I_{sAHP}). The key steps between calcium influx and potassium channel activation remain unknown. Here, we report that the key intermediate between calcium and the sAHP channels is the diffusible calcium sensor hippocalcin. Brief depolarizations sufficient to activate the I_{sAHP} in wild-type mice do not elicit the I_{sAHP} in *hippocalcin* knockout mice. Introduction of hippocalcin in cultured hippocampal neurons leads to a pronounced I_{sAHP} while neurons expressing a hippocalcin mutant, lacking N-terminal myristoylation, exhibit a small I_{sAHP} that is similar to that recorded in uninfected neurons. This implies hippocalcin must bind to the plasma membrane to mediate its effects. These findings support a model in which the calcium sensor for the sAHP channels is not pre-associated with the channel complex.

INTRODUCTION

In the brain, calcium prevents runaway neuronal activity and seizures by activating potassium channels to dampen neuronal excitability. In adapting neurons, this leads to a pronounced afterhyperpolarization and consequently spike frequency adaptation. The afterhyperpolarization is subdivided into three phases: fast (fAHP), medium (mAHP), and slow (sAHP). Unlike the fAHP and mAHP that last for a few seconds, the sAHP hyperpolarizes the neurons for many seconds and is highly regulated by neurotransmitters and neuromodulators such as norepinephrine, glutamate, acetylcholine, and serotonin (Nicoll, 1988). Although the sAHP has been extensively studied for the past three decades, both the potassium channel underlying the sAHP and the mechanism of calcium activation remain unknown (Vogalis et al., 2003).

The emerging view of calcium gating of potassium channels is that calcium directly gates the channels by binding either to a calcium sensor intrinsic to the potassium channels (i.e. BK channels) or a calcium sensor covalently tethered to the channels (i.e. SK channels). Calcium

*Address all correspondence to: Roger A. Nicoll, Department of Cellular and Molecular Pharmacology, University of California San Francisco, CA 94143, Phone: (415) 476-2018, E-mail: nicoll@cmp.ucsf.edu.

activated potassium channels are also pre-associated with calcium channels, scaffolding molecules, and signal transduction proteins (Bekerfeld et al, 2006; Levitan, 2006). Overall, this data support a model in which calcium-activated potassium channels are part of a large membrane delimited macromolecular complex that leads to the formation of calcium signaling in micro- and nano- domains.

Here, we provide evidence that the calcium gating of the sAHP potassium channels does not conform to the classical model of potassium channel gating by calcium. First, we show that the calcium chelators EGTA and BAPTA modulate the current kinetics of the sAHP channels and the apamin SK channels in an opposite manner, suggesting that the calcium gating of the sAHP and SK channels is through different mechanisms. Next, we propose that the diffusible neuronal calcium sensor hippocalcin is the critical protein in the calcium gating of the sAHP channels, as brief depolarizations do not lead to the activation of the I_{sAHP} in *hippocalcin* knockout mice. Finally, neurons in culture virally infected with hippocalcin exhibit a robust sAHP, unlike uninfected neurons, or neurons infected with a hippocalcin mutant that cannot associate to the plasma membrane. Our data support a novel calcium signaling mechanism that allows for neurons to integrate the calcium signal across the entire cell and not only in nano- or micro- domains.

RESULTS AND DISCUSSION

Calcium transients in response to a brief depolarization to activate voltage-gated calcium channels peak and decay faster than the activation and deactivation kinetics of the sAHP. (Abel et al., 2004; Jahromi et al., 1999; Sah and Clements, 1999). Several theories have been proposed to explain this disparity: (1) the slow sAHP kinetics may reflect diffusion of calcium from voltage-gated calcium channels to sAHP channels (Lancaster and Zucker, 1994). (2) Alternatively, calcium-activated potassium channels with high affinity for calcium, but with slow binding and unbinding kinetics may gate the sAHP (Sah and Clements, 1999). (3) Calcium may engage an intracellular intermediate that in turn activates sAHP channels (Abel et al., 2004; Gerlach et al., 2004).

To distinguish among these possibilities, we compared the effects of different calcium buffers on the kinetics of the I_{sAHP} and the apamin-sensitive SK component of the medium AHP ($I_{SK\text{-}AHP}$). SK channels are calcium activated potassium channels with constitutively bound calmodulin acting as their calcium sensor (Xia et al., 1998). Therefore, if the sAHP is activated through a similar mechanism, calcium buffers should have qualitatively the same effect on both channels.

To isolate $I_{SK\text{-}AHP}$ from the total depolarization induced I_{AHP}, 100 nM apamin is bath applied to produce an irreversible complete block of SK channels (Stocker, 2004). Currents in the presence of apamin were subtracted from those without apamin to determine $I_{SK\text{-}AHP}$. The slow current remaining in apamin reflects the I_{sAHP} (Figure 1A right). In the presence of either 0.5 mM EGTA or 0.5 mM BAPTA, the $I_{SK\text{-}AHP}$ decays much faster than in the absence of any added calcium buffers (Figure 1B; Sah, 1992). In contrast, the I_{sAHP} decay kinetics do not change in the presence of 0.5 mM EGTA and they are significantly prolonged in the presence of 0.5 mM BAPTA (Figure 1C). Higher concentrations of BAPTA (1 mM) slow the I_{sAHP} kinetics even further (data not shown; $\tau_{decay} = 9.31 \pm 1.3$ s, n=4; (Sah and Clements, 1999) as do higher concentrations of EGTA (2 mM; Sah and Clements, 1999).

What accounts for the difference between $I_{SK\text{-}AHP}$ and I_{sAHP} when exogenous buffers are introduced? Upon activation of voltage-gated calcium channels, calcium clouds expand radially from the membrane towards the intracellular space away from the calcium channels. This leads to an approximately exponential decay of the calcium concentration at the membrane

following calcium channel closure. The decay of the calcium transient depends on the endogenous calcium buffers and calcium uptake/extrusion mechanisms (Neher, 1998). EGTA and BAPTA are mobile calcium buffers that accelerate the decay of calcium at the membrane, but prolong calcium clearance from the intracellular space (Dargan and Parker, 2003; Sah and Clements, 1999). Therefore, one interpretation for the difference between $I_{SK\text{-}AHP}$ and I_{sAHP} is that $I_{SK\text{-}AHP}$ reports the peak calcium concentration in close proximity to the calcium channels and its decay away from the membrane, while I_{sAHP} reflects the buildup of calcium in the intracellular space. A prediction of this model is that the I_{sAHP} will depend on the rate of calcium accumulation in intracellular compartments. Accordingly, the time-to-peak of the I_{sAHP} (662 ± 46 ms, n=7) in the presence of either 0.5 mM EGTA (1051 ± 113 ms, n=6; $p<0.01$ ANOVA) or 0.5 mM BAPTA (1602 ± 63 ms, n=5; $p<.0001$ ANOVA) is significantly delayed compared to control conditions (Figure 1C left; see also Jahromi et al., 1999; Lancaster and Zucker, 1994; Sah and Clements, 1999; Zhang et al., 1995). This is in contrast to the peak latency of the $I_{SK\text{-}AHP}$ (Figure 1B; 0 mM buffer: 22.06 ± 3 ms, n=7; 0.5 mM EGTA: 18.3 ± 3 ms, n=5 p=0.68; 0.5 mM BAPTA: 14.6 ± 3 ms, n=5, p=0.25 ANOVA). This implies that the slowing of the I_{sAHP} peak latency is due to the longer time it takes for calcium to reach equilibrium in the presence of EGTA and BAPTA (Lee et al., 2000). Further supporting our hypothesis that the buildup of calcium in the intracellular space triggers the I_{sAHP}, I_{sAHP} induction closely parallels global cytosolic calcium concentration (Abel et al., 2004; Knopfel et al., 1990) while $I_{SK\text{-}AHP}$ does not (Abel et al., 2004).

If the I_{sAHP} depends on the buildup of calcium entering the neuron, then a diffusible intermediate that relays the increase of intracellular calcium to the sAHP potassium channels may be involved. One candidate is the multifunctional calcium sensor calmodulin. However, we do not favor calmodulin as the critical intermediate for the following reasons: (1) In most ion channels modulated by calmodulin, calmodulin is part of the channel complex even in the apostate (Bradley et al, 2004; Erickson et al., 2001; Wen and Levitan, 2002; Xia et al., 1998). (2) The I_{sAHP} has a calcium affinity of 200 nM, which is higher than the affinities of potassium channels modulated by calmodulin (Stocker, 2004). Other possible candidates for intermediates between calcium and sAHP include members of the Neuronal Calcium Sensor (NCS) protein family.

The NCS family is comprised of a large number of proteins known to regulate synaptic plasticity (Palmer et al, 2005) and the activity of ion channels including potassium and calcium channels (An et al., 2000; Few et al., 2005). Hippocalcin, a member of this protein family, is highly enriched in hippocampus and is found in cortical areas with prominent sAHPs (Kobayashi et al., 2005; Paterlini et al., 2000). The I_{sAHP} and hippocalcin share similar calcium sensitivity (Ca threshold for activation: ~160 nM vs ~180 nM and Ca K_m: ~200 nM vs ~290 nM, respectively; Abel et al., 2004; O'Callaghan et al., 2003). In addition, following a train of action potentials, hippocalcin associates with the plasma membrane in cultured hippocampal neurons (Belan et al., 2005). Binding of calcium to hippocalcin promotes a conformational change that exposes a myristoyl moiety (calcium myristoyl switch; Kobayashi et al., 1993; O'Callaghan et al., 2003). This allows hippocalcin to associate with the plasma membrane thereby shifting hippocalcin from a freely diffusible cytosolic protein to a membrane-bound protein.

To examine a possible role of hippocalcin in modulating the activity of the I_{sAHP}, we assayed the $I_{SK\text{-}AHP}$ and the I_{sAHP} in hippocampal slices prepared from either wild-type ($HC^{+/+}$) or *hippocalcin* knockout ($HC^{-/-}$) mice in a blind study (Kobayashi et al., 2005; Korhonen et al., 2005) (Figure 2). Consistent with hippocalcin being a high affinity calcium binding protein, the $I_{SK\text{-}AHP}$ in slices from $HC^{-/-}$ mice had larger peak amplitudes (Figure 2A; 149.1 ± 11 pA, n=15; $p<0.05$ Students-t-test) than those from $HC^{+/+}$ slices (114.9 ± 4.9 pA, n=10). To control for differences in $I_{SK\text{-}AHP}$ kinetics we measured the charge transfer through the $I_{SK\text{-}AHP}$. Like

the peak amplitudes, we found that the time integral was doubled in the $HC^{-/-}$ mice ($HC^{+/+}$: 37.9 ± 5.9 pC, n=10; $HC^{-/-}$: 68.5 ± 9.2 pC, n=15; p<0.05 Students-t-test). Thus, with respect to I_{SK-AHP}, hippocalcin acts as a calcium buffer. In contrast, the I_{sAHP} is not readily observable in slices prepared from $HC^{-/-}$ mice even in neurons with a robust I_{SK-AHP} (Figure 2B). Compromised calcium handling in $HC^{-/-}$mice could explain our data. However, the increased peak amplitude of SK currents argues against this possibility.

The amplitude of the sAHP depends on the duration of the depolarizing pulse used to induce the sAHP (Madison and Nicoll, 1984), suggesting that hippocalcin may set the threshold for sAHP activation. Indeed, increasing the duration of the stimulus from 100 ms to 300 ms induces a larger I_{sAHP} in $HC^{-/-}$ slices. In a blind study, the I_{sAHP} following a long depolarizing pulse (300 ms) was 51.05 ± 5.01 pA (n=28) in slices prepared from $HC^{+/+}$ mice, while the I_{sAHP} in slices prepared from $HC^{-/-}$ mice was only 27.9 ± 2.4 pA (n=31; p<.0001; Student's-t-test; i.e. 50% reduced). A summary of the I_{sAHP}s from either $HC^{+/+}$ or $HC^{-/-}$ mice evoked using different depolarizing pulse durations is shown in figure 3A. Notice, that at all stimulus durations the I_{sAHP} from $HC^{-/-}$ mice is significantly smaller than the I_{sAHP} recorded in $HC^{+/+}$ mice.

The need to use long duration pulses (300 ms) to induce I_{sAHP} in $HC^{-/-}$ mice raises the question of whether I_{sAHP}s recorded in $HC^{-/-}$ mice has properties similar to the I_{sAHP} recorded in $HC^{+/+}$ mice. Like the I_{sAHP} in $HC^{+/+}$ mice, the I_{sAHP} in $HC^{-/-}$ mice induced by a long depolarizing pulse (300 ms) has slow kinetics ($HC^{+/+}$: 3.82 ± 0.17 s, n=28; $HC^{-/-}$: 3.36 ± 0.22 s, n=31; p=0.11 Student's t-test) and is blocked by the inorganic non-selective voltage-gated calcium channel blocker cadmium (data not shown; $HC^{+/+}$: 88.7 ± 2 % block, n=4; $HC^{-/-}$: 79.8 ± 5 % block, n=3). Another hallmark of the sAHP is its selective inhibition by norepinephrine (NE) through beta 1-noradrenergic receptors (Madison and Nicoll, 1982). In $HC^{-/-}$ mice, the block of the I_{sAHP} by NE following a long depolarizing pulse (300 ms) is significantly smaller than that in $HC^{+/+}$ mice (Figure 3B). Thus, although long duration depolarizing pulses in $HC^{-/-}$ mice induce a I_{sAHP} that is ~50% of the $HC^{+/+}$ I_{sAHP}, the NE sensitive I_{sAHP} is even further reduced to ~30% of the $HC^{+/+}$ I_{sAHP} (NE sensitive current: $HC^{+/+}$: 32.5 ± 3.8 pA, n=14; $HC^{-/-}$: 11.7 ± 3.5, n=16; p<0.001 Students-t-test).

Together our data suggest that hippocalcin is the key intermediate step in the signal transduction cascade between intracellular calcium and generation of the NE sensitive I_{sAHP}. Upon calcium binding to hippocalcin, a myristoyl moiety is exposed that allows hippocalcin to bind the plasma membrane (O'Callaghan et al., 2002; O'Callaghan et al., 2003). A close homologue of hippocalcin, VILIP-2, also found in hippocampus, modulates calcium channels by relieving calcium-induced inactivation. To exert its effect VILIP-2 has to associate with the plasma membrane by utilizing the calcium myristoyl switch (Few et al., 2005). To test whether hippocalcin must be membrane bound to modulate I_{sAHP}, we used dissociated neurons kept in culture for 8–9 days. Previous studies have reported difficulty in recording I_{sAHP} in dissociated neuronal cultures (Alger et al., 1994) or that the I_{sAHP} runs down within a few minutes of using standard electrophysiological techniques (Shah and Haylett, 2000).

To examine the functional role of hippocalcin myristoylation in generating the I_{sAHP} we used a mutant, HC^{G2A}, in which the normally myristoylated glycine is mutated to an alanine. This mutation is known to prevent N-terminal myristoylation of hippocalcin (O'Callaghan et al., 2002; O'Callaghan et al., 2003). Similar to previous reports, uninfected neurons have little or no I_{sAHP} (Figure 4). However, neurons infected with wild-type hippocalcin (HC^{wt}) show a robust I_{sAHP}, while neurons infected with a hippocalcin mutant (HC^{G2A}) that cannot bind to the plasma membrane have an I_{sAHP} that is similar to the I_{sAHP} recorded in uninfected neurons (Figure 4). Therefore, like VILIP-2, hippocalcin must bind to the plasma membrane to induce its modulation.

The prevailing view of potassium channel activation by calcium is that it is membrane delimited. That is, the potassium channels, the calcium sensor, and in some cases the calcium channels are pre-assembled in a macromolecular protein complex (Berkerfeld et al, 2006; Levitan et al, 2006). This results to the formation of signaling nano- and micro-domains, which are necessary for neurotransmission release and rapid repolarization of the membrane following action potentials. However, pre-association of potassium channels with the calcium sensor would also dissociate the potassium channels from detecting any changes in the global calcium levels.

Here, we show that the neuronal calcium sensor hippocalcin, which is not associated with the channel complex, gates the potassium channel that mediates the slow afterhyperpolarization. Thus, the I_{sAHP} is greatly reduced in hippocampal slices from *hippocalcin* knockout mice. Furthermore, expression of wild-type hippocalcin in dissociated neurons, but not a hippocalcin mutant lacking the myristoyl moiety, markedly enhances I_{sAHP}. The latter finding indicates that movement of hippocalcin from the cytosol to the membrane is a necessary step in the gating of the I_{sAHP}. Our findings strongly suggest that the I_{sAHP} channels respond to a global rise in cytosolic calcium and that an intermediary step is required to relay the signal back to the membrane. Hippocalcin is ideally suited for this intermediary step, since it binds cytosolic calcium and then binds to the cell membrane, via a calcium myristoyl switch.

A number of issues remain unresolved. Although I_{sAHP} is greatly reduced in *hippocalcin* knockout mice, a small I_{sAHP} can still be detected in response to prolonged depolarizing pulses. As low concentrations of BAPTA (0.5 mM) also prolong the I_{sAHP} kinetics in *hippocalcin* knockout mice (data not shown), perhaps one of the numerous other diffusible neuronal calcium sensors accounts for this remaining current. How does hippocalcin activate I_{sAHP} channels? Previously it has been shown that the calcium neuronal sensor KChIP binds directly to the cytoplasmic amino termini of A-type potassium channels and modulates their kinetics in a calcium dependent manner (An et al, 2000). Perhaps a similar mechanism may account for hippocalcin's activation of the sAHP channels. Are *hippocalcin* knockout mice hyperexcitable, as might be expected, from the loss of the sAHP? Although hippocalcin levels decrease during epileptogenesis (Elliott et al, 2003), to date, no studies have addressed whether or not *hippocalcin* knockout mice are susceptible to seizures. However, the increase in calcium activation of SK channels (Figure 2) or other calcium activation processes might compensate for the sAHP loss. Regardless what the answers to these questions may be, the mechanism uncovered in this study allows the channels underlying the I_{sAHP} to integrate calcium changes across the entire cell and thus respond to overall changes in neuronal excitability.

EXPERIMENTAL PROCEDURES

Experiments were carried out according to the guidelines of the UCSF Committee of Animal Research.

Knocout mice and PCR genotyping

The hippocalcin knockout mice ($HC^{-/-}$) were maintained by breeding $HC^{-/-}$ males and females. The $HC^{-/-}$ mice were backcrossed to C57Bl/6 backround eight times (see (Kobayashi et al., 2005; Korhonen et al., 2005) for details on generation and description of $HC^{-/-}$ mice). PCR genotyping of the mouse tail prep DNA was performed as described previously (Kobayashi et al., 2005) using the following primers: (1) 5′-ACTGGCTCCTCAGCCTTTGTCTCTGA ACAC-3′, (2) 5′-TCGTGCTTTACGGTATCGCCGCTCCCGATT-3′, (3) 5′-TAGCCAGAGCTATGTAGTGA GATCCTGTCTC-3′.

Recordings and Solutions

Briefly, transverse hippocampal slices (300–400 μm) were prepared from 16 to 22 day-old hippocalcin knockout and wild-type mice. Animals were decapitated, and the hippocampus was dissected out and glued to the stage of a vibroslicer (Leica Instruments) in ice-cold artificial cerebrospinal fluid (ACSF) (in mM): 119 NaCl, 2.5 KCl, 1.3 $MgSO_4$, 2.5 $CaCl_2$, 1 NaH_2PO_4, 26 $NaHCO_3$, 10 glucose; equilibrated with 95% O_2 and 5% CO_2. Slices were maintained at 35 °C (30 min) and then at room temperature in a storage chamber that was continuously perfused with ACSF for at least 1 hr prior to recordings. Whole-cell recordings were made with infrared differential interference contrast optics using a ×40 water-immersion objective on an upright microscope (Olympus BX50). Pipettes with resistances of 3 to 4 MΩ were used. The series resistance, as measured by the instantaneous current response to a 4 mV step with only the pipette capacitance canceled, was always less than 30 MΩ. Pipette solutions contained (in mM) 150 potassium methylsulfate, 10 KCl, 10 HEPES, 4 NaCl, 4 Mg_2ATP, and 0.4 Na_4GTP. Osmolarity was adjusted to 290–300 mOsm/l and pH to 7.25–7.35 with KOH. The slices were bathed in a modified ACSF containing 500 nM TTX to block voltage gated sodium channels. Responses following depolarizing pulses of varying durations (see text) were collected with an Axopatch-1D amplifier, filtered at 2 kHz, digitized at 5 kHz and analysed on line using Igor Pro software (Wavemetrics, Lake Oswego, OR, USA). Statistical significance was determined using either variance analysis (ANOVA) with Tukey as a post hoc test or unpaired Student's-t-test.

Dissociated neurons and Viral Infection

Dissociated hippocampal cultures were prepared from P0 Sprague-Dawley rat pups as described previously (Adesnik et al., 2005). Cultures were used for physiology between 8–9 DIV. For viral infection of rat dissociated neurons Hippocalcin-EGFP and G2A-EGFP were subcloned into pSCA1 and viral particles were generated by transfecting pSCA1-Hippocalcin (or G2A)-EGFP and pHelper into HEK293 cells. After 48–72hrs following transfection supernatants were harvested, aliquoted and stored −80°C. Prior to infection, the viral particles were activated with chymotrypsin. For infection, viral solutions were added to rat dissociated neurons that were 8–9 DIV. A depolarizing pulse (150 ms) to +15 mV from a holding membrane potential of −50 mV is used to induce the I_{sAHP} in dissociated cultured neurons (Shah and Haylett, 2000).

Acknowledgements

We thank V. Stein for expert technical assistance with viral infections and subcloning, J. I. Wadiche, Karen Menuz, Kim Moore, Olav Olsen, and all members of the Nicoll lab for discussions. We also thank Dr. R.D. Burgoyne for the hippocalcin constructs. This work was funded by NIH grants to R.A.N and AHA postdoctoral fellowship to A.V.T.

References

Abel HJ, Lee JC, Callaway JC, Foehring RC. Relationships between intracellular calcium and afterhyperpolarizations in neocortical pyramidal neurons. J Neurophysiol 2004;91:324–335. [PubMed: 12917389]

Adesnik H, Nicoll RA, England PM. Photoinactivation of native AMPA receptors reveals their real-time trafficking. Neuron 2005;48:977–985. [PubMed: 16364901]

Alger BE, Sim JA, Brown DA. Single-channel activity correlated with medium-duration, Ca-dependent K current in cultured rat hippocampal neurones. Neurosci Lett 1994;168:23–28. [PubMed: 8028783]

An WF, Bowlby MR, Betty M, Cao J, Ling HP, Mendoza G, Hinson JW, Mattsson KI, Strassle BW, Trimmer JS, Rhodes KJ. Modulation of A-type potassium channels by a family of calcium sensors. Nature 2000;403:553–556. [PubMed: 10676964]

Berkerfeld H, Sailer CA, Bildl W, Rohde V, Thumfart JO, Eble S, Klugbauer N, Reisinger E, Bischofberger J, Oliver D, Knaus HG, Schulte U, Fakler B. BKCa-Cav channel complexes mediate rapid and localized Ca2+-activated K+ signaling. Science 2006;314:615–20. [PubMed: 17068255]

Belan P, Markova O, Fitzgerald D, Stepanyuk A, Tsugorka T, Drebot Y, Tepikin A, Burgoyne RD. Hippocalcin as a possible messenger in site-specific, short-term signal transduction in the hippocampus. Soc Neurosci Abst. 2005Program N0. 610.14

Bradley J, Bonigk W, Yau KW, Frings S. Calmodulin permanently associates with rat olfactory CNG channels under native conditions. Nat Neurosci 2004;7:705–10. [PubMed: 15195096]

Dargan SL, Parker I. Buffer kinetics shape the spatiotemporal patterns of IP3-evoked Ca2+ signals. J Physiol 2003;553:775–788. [PubMed: 14555715]

Elliott RC, Miles MF, Lowenstein DH. Overlapping microarray profiles of dentate gyrus gene expression during development- and epilepsy-associated neurogenesis and axon outgrowth. J Neurosci 2003;23:2218–27. [PubMed: 12657681]

Erickson MG, Alseikhan BA, Peterson BZ, Yue DT. Preassociation of calmodulin with voltage-gated Ca(2+) channels revealed by FRET in single living cells. Neuron 2001;31:973–985. [PubMed: 11580897]

Few AP, Lautermilch NJ, Westenbroek RE, Scheuer T, Catterall WA. Differential regulation of CaV2.1 channels by calcium-binding protein 1 and visinin-like protein-2 requires N-terminal myristoylation. J Neurosci 2005;25:7071–7080. [PubMed: 16049184]

Gerlach AC, Maylie J, Adelman JP. Activation kinetics of the slow afterhyperpolarization in hippocampal CA1 neurons. Pflugers Arch 2004;448:187–196. [PubMed: 14727118]

Jahromi BS, Zhang L, Carlen PL, Pennefather P. Differential time-course of slow afterhyperpolarizations and associated Ca2+ transients in rat CA1 pyramidal neurons: further dissociation by Ca2+ buffer. Neuroscience 1999;88:719–726. [PubMed: 10363812]

Knopfel T, Vranesic I, Gahwiler BH, Brown DA. Muscarinic and beta-adrenergic depression of the slow Ca2(+)-activated potassium conductance in hippocampal CA3 pyramidal cells is not mediated by a reduction of depolarization-induced cytosolic Ca2+ transients. Proc Natl Acad Sci U S A 1990;87:4083–4087. [PubMed: 2161530]

Kobayashi M, Masaki T, Hori K, Masuo Y, Miyamoto M, Tsubokawa H, Noguchi H, Nomura M, Takamatsu K. Hippocalcin-deficient mice display a defect in cAMP response element-binding protein activation associated with impaired spatial and associative memory. Neuroscience 2005;133:471–484. [PubMed: 15878804]

Kobayashi M, Takamatsu K, Saitoh S, Noguchi T. Myristoylation of hippocalcin is linked to its calcium-dependent membrane association properties. J Biol Chem 1993;268:18898–18904. [PubMed: 8360179]

Korhonen L, Hansson I, Kukkonen JP, Brannvall K, Kobayashi M, Takamatsu K, Lindholm D. Hippocalcin protects against caspase-12-induced and age-dependent neuronal degeneration. Mol Cell Neurosci 2005;28:85–95. [PubMed: 15607944]

Lancaster B, Zucker RS. Photolytic manipulation of Ca2+ and the time course of slow, Ca(2+)-activated K+ current in rat hippocampal neurones. J Physiol 1994;475:229–239. [PubMed: 8021830]

Lee SH, Schwaller B, Neher E. Kinetics of Ca2+ binding to parvalbumin in bovine chromaffin cells: implications for [Ca2+] transients of neuronal dendrites. J Physiol 2000;525(Pt 2):419–432. [PubMed: 10835044]

Levitan IB. Signaling protein complexes associated with neuronal ion channels. Nat Neurosci 2006;9:305–10. [PubMed: 16498425]

Madison DV, Nicoll RA. Noradrenaline blocks accommodation of pyramidal cell discharge in the hippocampus. Nature 1982;299:636–638. [PubMed: 6289127]

Madison DV, Nicoll RA. Control of the repetitive discharge of rat CA 1 pyramidal neurones in vitro. J Physiol 1984;354:319–331. [PubMed: 6434729]

Neher E. Usefulness and limitations of linear approximations to the understanding of Ca++ signals. Cell Calcium 1998;24:345–357. [PubMed: 10091004]

Nicoll RA. The coupling of neurotransmitter receptors to ion channels in the brain. Science 1988;241:545–551. [PubMed: 2456612]

O'Callaghan DW, Ivings L, Weiss JL, Ashby MC, Tepikin AV, Burgoyne RD. Differential use of myristoyl groups on neuronal calcium sensor proteins as a determinant of spatio-temporal aspects of Ca2+ signal transduction. J Biol Chem 2002;277:14227–14237. [PubMed: 11836243]

O'Callaghan DW, Tepikin AV, Burgoyne RD. Dynamics and calcium sensitivity of the Ca2+/myristoyl switch protein hippocalcin in living cells. J Cell Biol 2003;163:715–721. [PubMed: 14638856]

Palmer CL, Lim W, Hastie PG, Toward M, Koronolchuk VI, Burbidge SA, Banting G, Collingridge GL, Isaac JT, Henley JM. Hippocalcin functions as a calcium sensor in hippocampal LTD. Neuron 2005;47:487–94. [PubMed: 16102532]

Paterlini M, Revilla V, Grant AL, Wisden W. Expression of the neuronal calcium sensor protein family in the rat brain. Neuroscience 2000;99:205–216. [PubMed: 10938426]

Sah P. Role of calcium influx and buffering in the kinetics of Ca(2+)-activated K+ current in rat vagal motoneurons. J Neurophysiol 1992;68:2237–2247. [PubMed: 1491269]

Sah P, Clements JD. Photolytic manipulation of [Ca2+]i reveals slow kinetics of potassium channels underlying the afterhyperpolarization in hippocampal pyramidal neurons. J Neurosci 1999;19:3657–3664. [PubMed: 10233997]

Shah M, Haylett DG. Ca(2+) channels involved in the generation of the slow afterhyperpolarization in cultured rat hippocampal pyramidal neurons. J Neurophysiol 2000;83:2554–2561. [PubMed: 10805657]

Stocker M. Ca(2+)-activated K+ channels: molecular determinants and function of the SK family. Nat Rev Neurosci 2004;5:758–770. [PubMed: 15378036]

Vogalis F, Storm JF, Lancaster B. SK channels and the varieties of slow after-hyperpolarizations in neurons. Eur J Neurosci 2003;18:3155–3166. [PubMed: 14686890]

Wen H, Levitan IB. Calmodulin is an auxiliary subunit of KCNQ2/3 potassium channels. J Neurosci 2002;22:7991–8001. [PubMed: 12223552]

Xia XM, Fakler B, Rivard A, Wayman G, Johnson-Pais T, Keen JE, Ishii T, Hirschberg B, Bond CT, Lutsenko S, et al. Mechanism of calcium gating in small-conductance calcium-activated potassium channels. Nature 1998;395:503–507. [PubMed: 9774106]

Zhang L, Pennefather P, Velumian A, Tymianski M, Charlton M, Carlen PL. Potentiation of a slow Ca (2+)-dependent K+ current by intracellular Ca2+ chelators in hippocampal CA1 neurons of rat brain slices. J Neurophysiol 1995;74:2225–2241. [PubMed: 8747186]

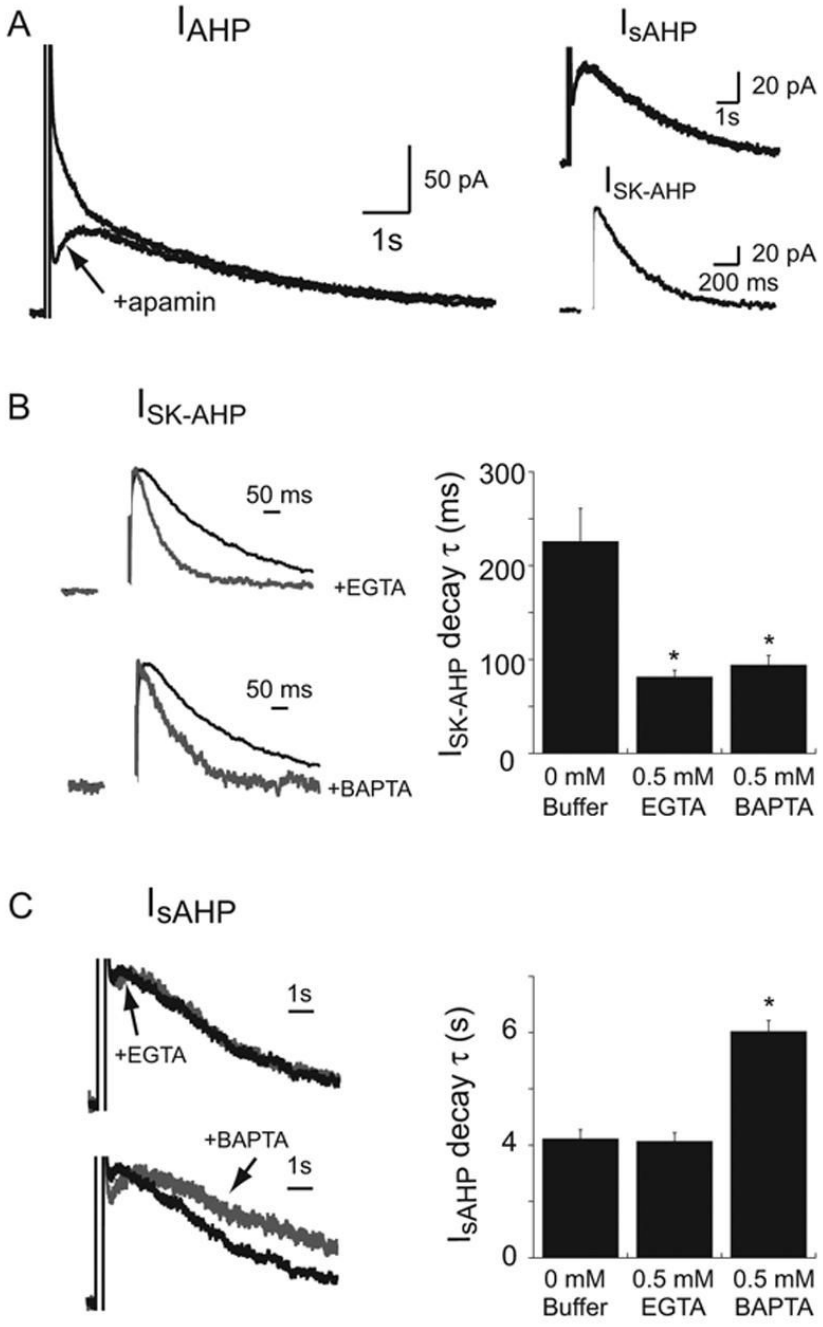

Figure 1. Calcium buffers differentially regulate the kinetics of the apamin-sensitive AHP current (I_{SK-AHP}) as compared to the sAHP current (I_{sAHP})

(A) Activation of the AHP current (I_{AHP}) and isolation of the I_{SK-AHP} and I_{sAHP}. Left, the currents underlying the AHP are recorded under voltage clamp in slices prepared from wild-type ($HC^{+/+}$) mice. I_{AHP} is triggered using a brief depolarizing voltage step from a holding membrane potential ($V_{holding}$) of −55 mV to +15 mV to activate voltage-gated calcium channels. Application of 100 nM apamin suppresses an early component of the I_{AHP}. Right, the pharmacologically isolated I_{SK-AHP} and I_{sAHP} is shown. Notice the different time scales. **(B)** Left, representative traces showing the I_{SK-AHP} in the absence of calcium buffers (black trace), in the presence of 0.5 mM EGTA, or in 0.5 mM BAPTA (gray trace). Traces are

normalized to their peak amplitude. Right, summary graph showing that the decay time constant of the $I_{SK\text{-}AHP}$ is faster in the presence of either 0.5 mM EGTA (81.25 ± 7.5 ms, n=5; p<.005) or 0.5 mM BAPTA (93.8 ± 11 ms, n=5, p<0.01) as compared to control $I_{SK\text{-}AHP}$ (225.6 ± 35 ms, n=7) recorded in the absence of any intracellular calcium buffers. **(C)** Left, representative traces showing the I_{sAHP} recorded in the absence of calcium buffers (black trace), in the presence of 0.5 mM EGTA, or in 0.5 mM BAPTA (gray trace). Traces are normalized to their peak amplitude. Right, graph summarizing the effect of 0.5 mM EGTA (4.13 ± 0.31 s, n=6; p=0.98) and 0.5 mM BAPTA (8.03 ± 0.39 s, n=5, p<.0001) on the I_{sAHP} decay kinetics as compared to control I_{sAHP} recorded in the absence of any intracellular calcium buffers (4.22 ± 0.33 s, n=7). Error bars show s.e.m.

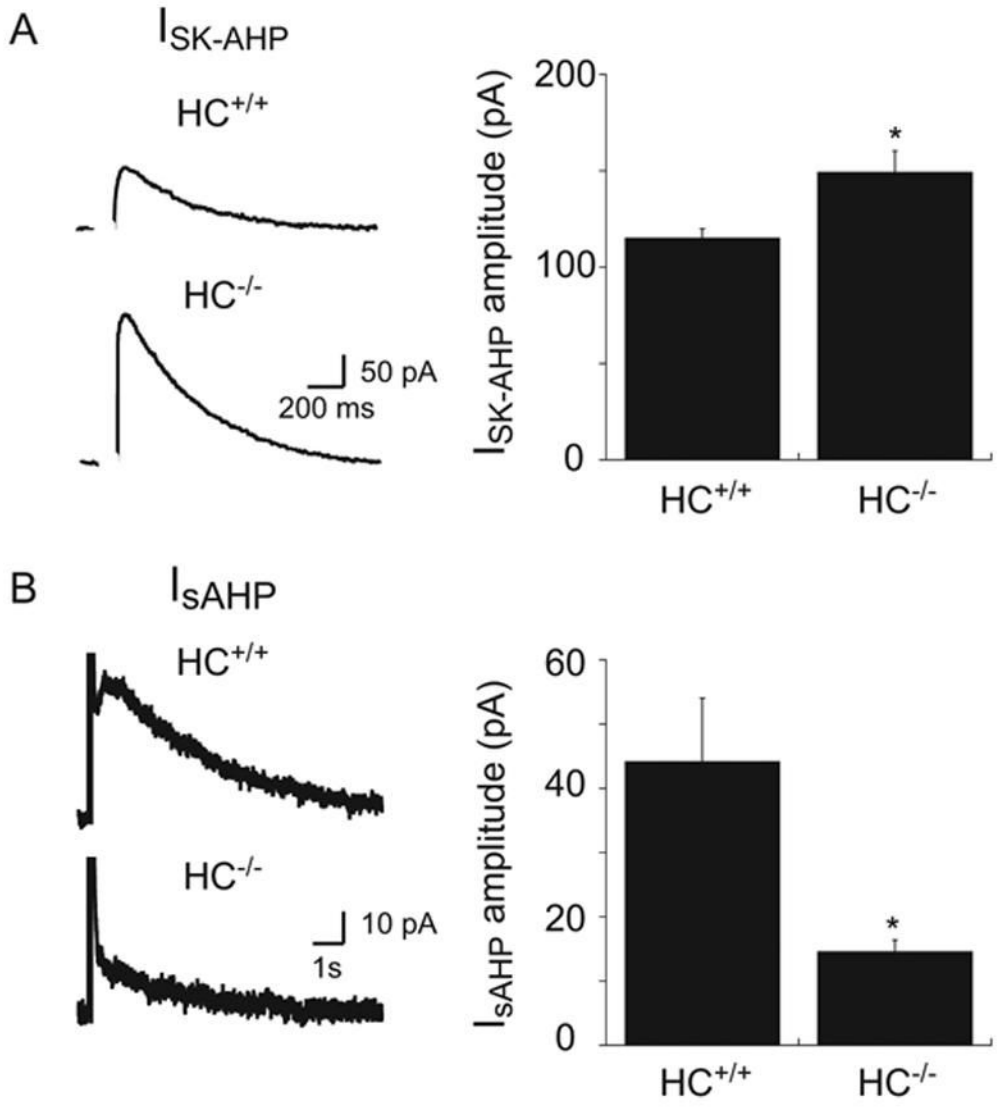

Figure 2. Loss of I_{sAHP} in slices prepared from hippocalcin knockout mice

(A) Left, traces of the current underlying the apamin sensitive AHP following a 100 ms depolarizing step to +15 mV from $V_{holding}$ of −55 mV in slices prepared from either $HC^{+/+}$ or *hippocalcin* knockout mice ($HC^{-/-}$). Right, summary graph showing the amplitude of I_{SK-AHP} is increased in slices prepared from $HC^{-/-}$ mice (149.1 ± 11 pA, n=15; $p<0.05$), as compared to slices from $HC^{+/+}$ mice (114.9 ± 4.9 pA, n=10). **(B)** Left, traces of the current underlying the sAHP from the same neurons and same stimulation protocol as described in A. Right, summary graph showing the amplitude of the I_{sAHP} is decreased in slices prepared from $HC^{-/-}$ mice (14.56 ± 1.86 pA, n=15; $p<.005$), as compared to slices from $HC^{+/+}$ mice (44.13 ± 9.9 pA, n=10). Error bars show s.e.m.

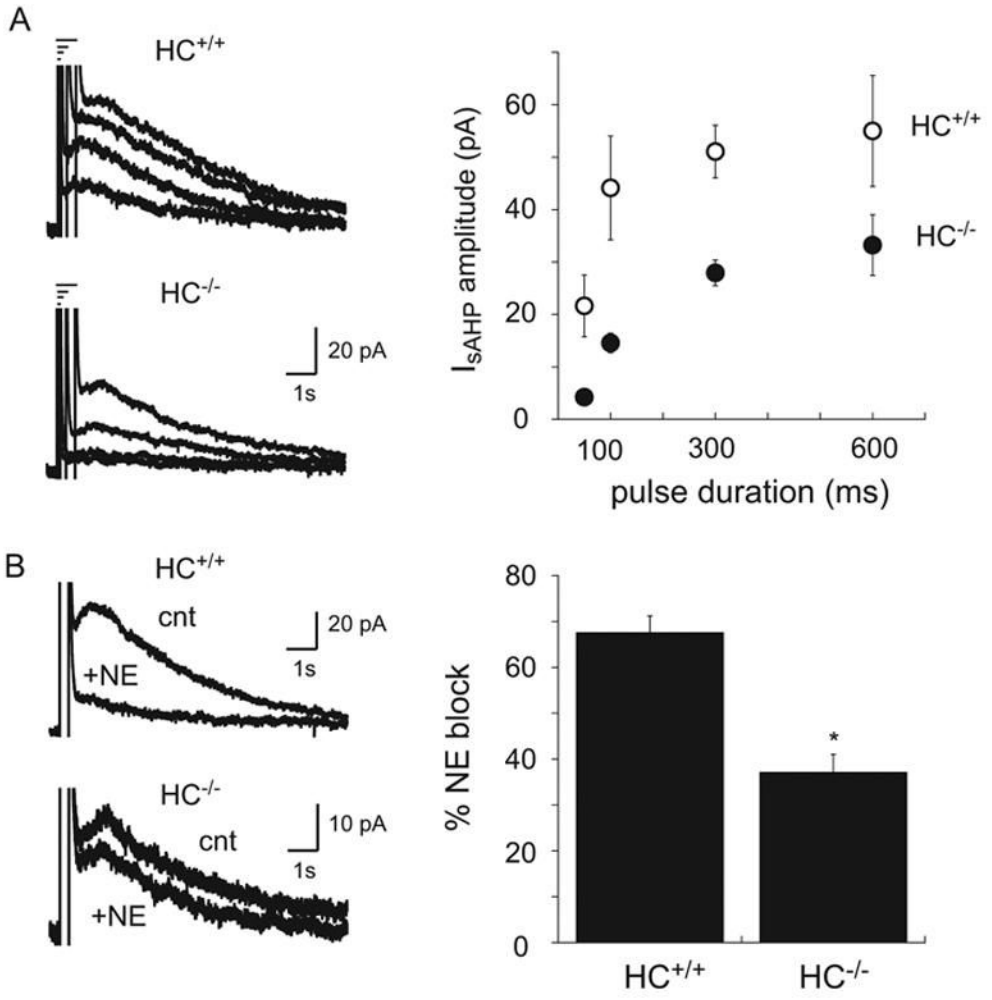

Figure 3. Long depolarizing pulses can evoke a I_{sAHP} in hippocalcin knockout mice that is largely norepinephrine insensitive

(A) Left top, representative traces from $HC^{+/+}$ mice that shows either short (50 ms or 100 ms) or long (300 ms or 600 ms) depolarizing pulses to +15 mV ($V_{holding}$ = −55 mV) evoke the I_{sAHP}. Left bottom, representative traces that shows only long (300 ms or 600 ms) depolarizing pulses to +15 mV ($V_{holding}$ = −55 mV) evoke the I_{sAHP} in $HC^{-/-}$ mice. Right, mean I_{sAHP} peak amplitude from either $HC^{+/+}$ or $HC^{-/-}$ mice in response to a depolarizing pulse to +15 mV ($V_{holding}$ = −55mV) of varying durations. The I_{sAHP} amplitude is significantly different between $HC^{+/+}$ and $HC^{-/-}$ mice for all pulse durations: 50 ms ($HC^{+/+}$: 21.6 ± 5.9 pA, n=5; $HC^{-/-}$: 3.81 ± 0.9 pA, n=7; p<0.01), 100 ms ($HC^{+/+}$: 43.4 ± 6.9 pA, n=15; $HC^{-/-}$: 12.1 ± 1.5 pA, n=24, p<.0001), 300 ms ($HC^{+/+}$: 52.9 ± 7.4, n=15; $HC^{-/-}$: 24.5 ± 2.3, n=24; p<.005), or 600 ms ($HC^{+/+}$: 55.00 ± 10.5 pA, n= 4; $HC^{-/-}$: 29.9 ± 5.2 pA, n=7; p<0.05) pulse duration.
(B) Left, representative traces of I_{sAHP} induced by a 300 ms depolarizing pulse to +15 mV ($V_{holding}$ = −55mV) before and after application of 20 μM norepinephrine in slices prepared from either $HC^{+/+}$ or $HC^{-/-}$ mice. Right, summary graph of the I_{sAHP} block induced by NE ($HC^{+/+}$: 67.5 ± 3.7 % block, n=16; $HC^{-/-}$: 37.1 ± 3.9 % block, n=14; p<.0001; Students-t-test). Error bars show s.e.m.

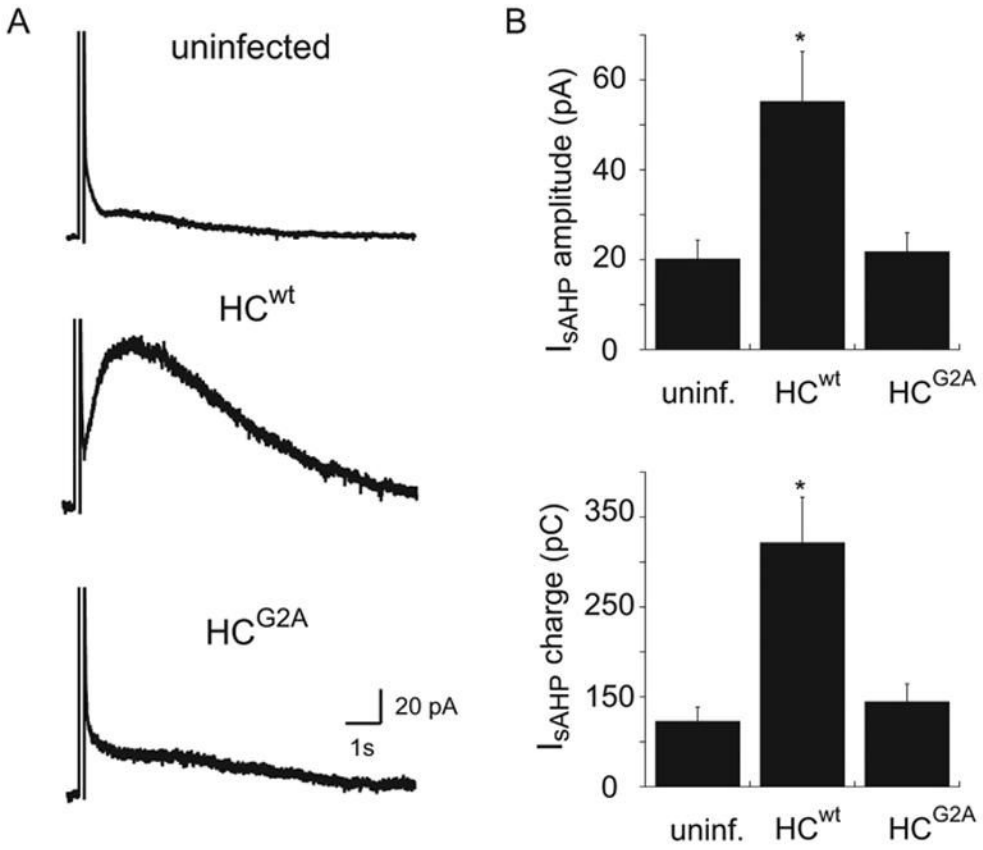

Figure 4. Myristoylation of hippocalcin is required for I_{sAHP} regulation

(A) Traces showing the dependence of I_{sAHP} on myristoylated hippocalcin. Top trace is from an uninfected neuron on a cover slip infected with wild-type hippocalcin. Middle panel shows a trace from an infected neuron expressing wild-type hippocalcin (HC^{wt}), while the bottom panel shows a neuron infected with HC^{G2A}, a mutant hippocalcin that cannot be myristoylated. (**B**) Top, graph summarizing the effect of expressing either HC^{wt} (55.2 ± 11 pA, n=16; p<0.01) or HC^{G2A} (21.8 ± 4.2 pA, n=16; p=0.98) to uninfected neurons (20.1 ± 4.3 pA, n=13) as measured by the peak I_{sAHP} amplitude. Bottom, graph summarizing the effect of expressing either HC^{wt} (271.2 ± 51 pC, n=16; p<0.001) or HC^{G2A} (94.3 ± 20.1 pC, n=16; p=0.9) to uninfected neurons (72.6 ± 15.9 pC, n=13) as measured by the area of the I_{sAHP} (350 ms following the end of the depolarizing pulse to 10 s). Error bars show s.e.m.